Spiking Neural Network Linear Equalization: Experimental Demonstration of 2km 100Gb/s IM/DD PAM4 Optical Transmission

Georg Böcherer[(1)], Florian Strasser[(1)], Elias Arnold[(2)], Youxi Lin[(1)], Johannes Schemmel[(2)], Stefano Calabrò[(1)], Maxim Kuschnerov[(1)]

[1] *Huawei Technologies Duesseldorf GmbH, Munich Research Center, Munich 80992, Germany*
[2] *Heidelberg University, Kirchhoff-Institute for Physics, Electronic Vision(s) Group, Heidelberg 69120, Germany*

[*] *georg.boecherer@ieee.org*

Abstract: A linear feed-forward equalizer is implemented by a potentially low-power spiking neural network. For a 100Gb/s PAM-4 IM/DD optical 2km transmission, no performance penalty compared to a digital implementation is observed.

1. Introduction

To sustain the exponential growth of data center traffic, optical transceivers need to evolve towards higher rates, smaller footprint and lower power consumption, at the same time. To achieve these challenging goals, recent research envisions moving parts of digital signal processing (DSP) to analog frontends with lower power consumption.

Photonic neuromorphic computing [1] has been proposed, e.g., for chromatic dispersion (CD) compensation and nonlinear equalization in short-reach optical transmission [2–4].

Also, a return to analog adaptive equalizers has gained traction, e.g., in [5], the transmitter DSP feeds two electrical non-return-to-zero (NRZ) signals to an analog pulse-amplitude-modulation 4-level (PAM-4) encoder, whose output is filtered by a continuous time linear equalizer (CTLE) and a 3-tap feed forward equalizer (FFE).

At the same time, the research community is striving to implement more powerful algorithms, e.g. based on artificial intelligence (AI) techniques, on analog electronics. An important subfield is in-memory-computing (IMC) [6], which aims for efficient calculation of vector-matrix multiplications. Research on IMC is mainly driven by the urgent need of AI accelerators for making inference by artificial neural networks (ANNs) more power-efficient. Eventually, IMC may enable the use of ANNs for signal processing in the data path of communication systems, see, e.g., [7]. Analog electronic neuromorphic computing offers an alternative path towards AI-based signal processing. Spiking neural networks (SNNs) [8] in analog hardware [9] combine IMC with sparse representation of information by spiking signals.

In [10, 11], we have shown by simulations in Norse [12] that SNN demappers compensate impairments in a simulated intensity-modulation / direct-detection (IM/DD) link, outperforming linear equalizers and nonlinear ANN equalizers. Using `hxtorch.snn` [13, Sec. 2.3.5], the proposed SNN demappers have been also mapped to and evaluated on the analog neuromorphic BrainScaleS-2 (BSS-2) hardware platform [9]. The simulated IM/DD link considered in [10, 11] is dominated by nonlinear impairments. In [14], SNN decision feedback equalization (DFE) is considered to compensate strong linear inter-symbol interference (ISI).

In this work, we consider offline processing of experimental data from a 100 Gb/s 2 km IM/DD PAM4 optical transmission link. We observe that after anti-alias filtering (AAF), timing recovery (TR), and downsampling, the received signal is mainly impaired by linear ISI. Hence, we propose the implementation of a linear FFE filter in a simple SNN. Despite the intrinsic nonlinearity of the spike mapping/demapping, the proposed SNN shows no performance penalty compared to a digital linear equalizer. This result promises significant power reduction, by dispensing with the analog-to-digital converter (ADC), and enabling sparse signaling and analog processing.

The remainder of this paper is organized as follows. In Sec. 2, we briefly introduce SNNs. We present the experimental setup in Sec. 3, and we conclude in Sec. 4 with a discussion of the results.

2. Spiking Neural Networks

In Fig. 1, we display SNNs as implemented in Norse [12]. Information is represented by spike trains $z_i(t) = \sum_k \delta(t - t_i^k)$ emitted by input neurons $\{n_i\}$. The spike trains are almost always equal to zero. Due to their sparsity, during one inference step, only a few neurons are active, and the active neurons only emit a small number of spikes, which results in very low power consumption. The input spike trains are then combined by a synaptic array, which calculates the weighted sum $\sum_i w_{ij} z_i(t)$. Subsequently, a filter with an impulse response that decays exponentially as $\exp(t/\tau_{\text{syn}})$ is applied, with τ_{syn} being the synaptic time constant. The resulting synaptic currents

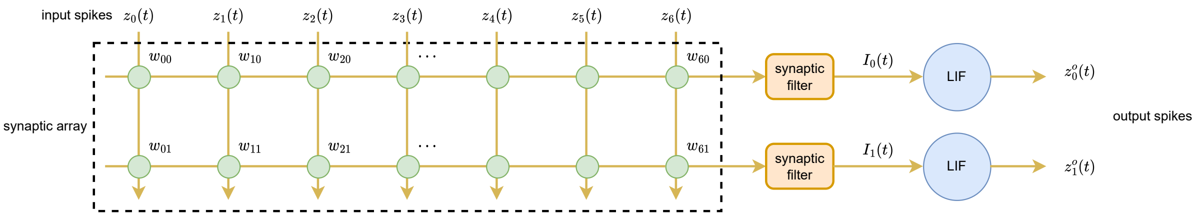

Fig. 1. SNN building block.

$I_j(t)$ are then fed to leaky-integrate and fire (LIF) neurons, which have as an internal state a membrane potential $v_j(t)$, described by the differential equation

$$\tau_{\mathrm{mem}} \dot{v}_j(t) = [v_\ell - v_j(t)] + R_\ell \cdot I_j(t), \tag{1}$$

where τ_m is the membrane time constant, v_ℓ a leakage potential, and R_ℓ the leakage resistance. When the membrane potential $v_j(t)$ exceeds a threshold v at time t_j^k, the LIF neuron emits a spike $z_j^o(t) = \delta(t - t_j^k)$ and the membrane potential is reset. Leaky-integrate (LI) neurons (not shown in the figure) follow the same dynamics as LIF neurons, without firing.

3. Experimental Setup

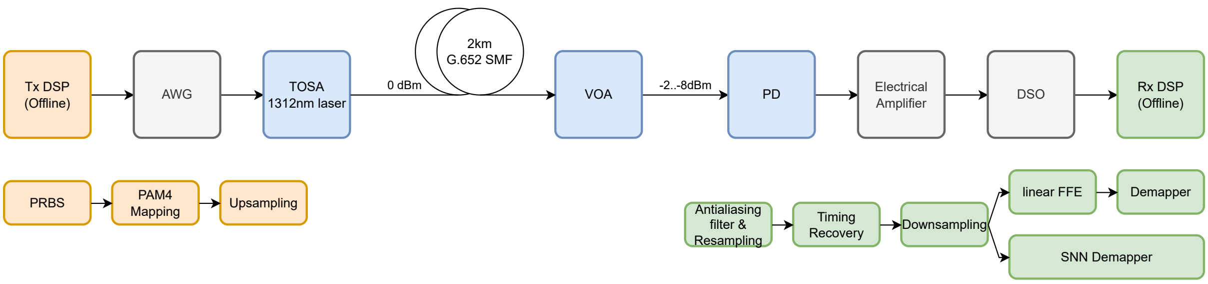

The experimental setup is displayed in the figure above. A pseudo-random bit sequence is generated offline and mapped to 256k PAM-4 symbols. The symbol sequence is then upsampled with NRZ pulse shaping to a 2 samples per symbol (SPS) sequence. The upsampled sequence is loaded to an arbitrary waveform generator (AWG) with a 3-dB bandwidth of >25 GHz. Assuming the 6% overhead KP4 forward error correction (FEC), we set the symbol rate to 53 GBd and operate the AWG at twice the symbol rate, i.e., 106 GSa/s, with the help of an external clock source. Afterwards, the electrical signal is fed to a transmitter optical sub-assembly (TOSA), which amplifies the electrical signal with an integrated driver amplifier and generates an optical signal with an electroabsorption modulated laser (EML). The TOSA output is fed into a 2km G.652 single-mode fiber (SMF). A variable optical attenuator (VOA) is used after the fiber to control the received optical power (ROP). A commercial receiver would detect the signal with a receiver optical sub-assembly (ROSA) containing a PIN photodiode (PD) and a phase-matched transimpedance amplifier (TIA). However, due to the unavailability of a ROSA during the experiment we use at the receiver a 70 GHz PIN PD accompanied by a 70 GHz 11 dB fixed gain electrical amplifier (EA). After the EA, the received electrical signal is quantized and captured with a digital storage oscilloscope (DSO) operating at 256 GSa/s with a 3-dB bandwidth of 113 GHz. By the VOA, we sweep the ROP at the PD input from -2 dBm to -8 dBm. After TR [15], the signal is downsampled to 1 sps and 4 M samples are stored for offline processing.

4. Results and Discussion

In Fig. 2, we compare a linear FFE followed by demapping with optimized decision boundaries with the proposed linear SNN demapping. For the considerd ROPs, the 1-tap linear FFE does not reach the KP4 threshold, which is in line with the substantial ISI that we expect from the spectrum displayed in Fig. 3. With a 9-tap linear FFE, we achieve a bit error rate (BER) below the KP4 threshold at -4 dBm.

Additionally, we consider a nonlinear ANN with two hidden layers with 40 and 20 neurons, respectively, and ReLU activations. An additional linear layer bypasses the hidden layers. The 4 ANN outputs are interpreted as log-probabilities on the four PAM4 symbols, corresponding to a soft decision (SD). The argmax of the SD provides the hard decision (HD). We note that nonlinear equalization improves only negligibly over the 9-tap linear FFE. Therefore, we conclude that the experimental link is mainly impaired by linear filtering effects and noise.

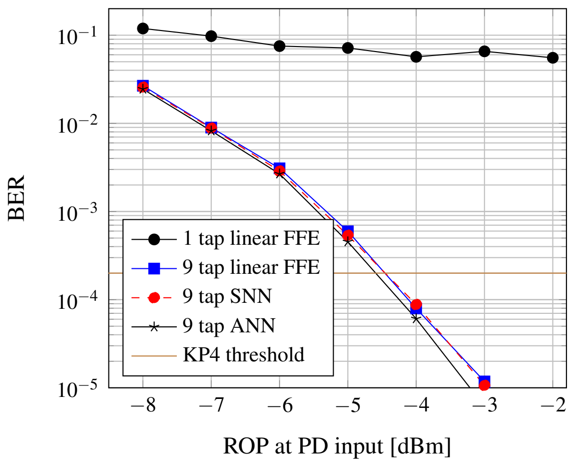

Fig. 2. BER results.

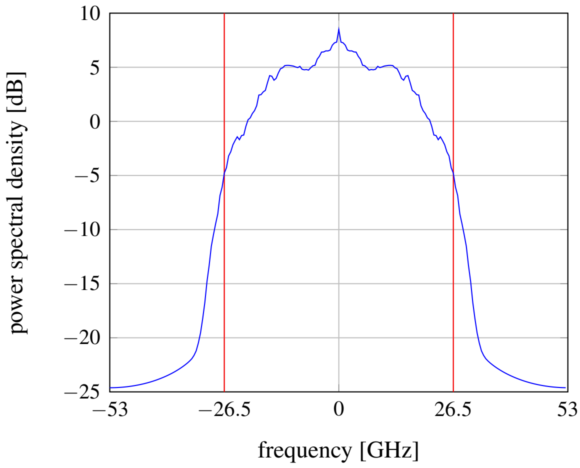

Fig. 3. Spectrum after AAF and resampling.

Conclusions. The proposed linear SNN performs exactly as well as the linear FFE, which shows that SNNs are a promising technology for low-power implementation of linear FFEs.

References

1. B. J. Shastri *et al.*, "Photonics for artificial intelligence and neuromorphic computing," *Nature Photonics*, 2021.
2. S. Li, S. Dev, S. Kühl, K. Jamshidi, and S. Pachnicke, "Micro-ring resonator based photonic reservoir computing for PAM equalization," *IEEE Photonics Technology Letters*, vol. 33, no. 18, pp. 978–981, 2021.
3. S. M. Ranzini, R. Dischler, F. Da Ros, H. Bülow, and D. Zibar, "Experimental investigation of optoelectronic receiver with reservoir computing in short reach optical fiber communications," *J. Lightw. Technol.*, vol. 39, no. 8, pp. 2460–2467, 2021.
4. K. Sozos, A. Bogris, P. Bienstman, and C. Mesaritakis, "Photonic reservoir computing based on optical filters in a loop as a high performance and low-power consumption equalizer for 100 Gbaud direct detection systems," in *2021 European Conference on Optical Communication (ECOC)*, pp. 1–4, IEEE, 2021.
5. G. Caruso, I. N. Cano, D. Nesset, G. Talli, and R. Gaudino, "Real-time 100Gb/s downstream PAM4 PON link with 34 dB power budget," in *European Conference on Optical Communication (ECOC)*, (Switzerland, Basel), Sept. 2022. Paper Tu4C.3.
6. G. W. Burr, R. M. Shelby, A. Sebastian, S. Kim, S. Kim, S. Sidler, K. Virwani, M. Ishii, P. Narayanan, A. Fumarola, *et al.*, "Neuromorphic computing using non-volatile memory," *Advances in Physics: X*, vol. 2, no. 1, pp. 89–124, 2017.
7. A. Eldebiky, G. Böcherer, G. L. Zhang, B. Li, M. Schädler, S. Calabrò, and U. Schlichtmann, "Power-efficient and robust nonlinear demapper for 64QAM using in-memory computing," in *European Conference on Optical Communication (ECOC)*, (Switzerland, Basel), Sept. 2022. Paper We3C.3.
8. W. Gerstner, W. M. Kistler, R. Naud, and L. Paninski, *Neuronal dynamics: From single neurons to networks and models of cognition*. Cambridge University Press, 2014.
9. C. Pehle, S. Billaudelle, B. Cramer, J. Kaiser, K. Schreiber, Y. Stradmann, J. Weis, A. Leibfried, E. Müller, and J. Schemmel, "The BrainScaleS-2 accelerated neuromorphic system with hybrid plasticity," *Frontiers in Neuroscience*, vol. 16, 2022.
10. E. Arnold, G. Böcherer, E. Müller, P. Spilger, J. Schemmel, S. Calabrò, and M. Kuschnerov, "Spiking neural network equalization for IM/DD optical communication," in *Optica Advanced Photonics Congress 2022*, Optica Publishing Group, 2022. Paper SpTu1J.2.
11. E. Arnold, G. Böcherer, E. Müller, P. Spilger, J. Schemmel, S. Calabrò, and M. Kuschnerov, "Spiking neural network equalization on neuromorphic hardware for IM/DD optical communication," in *Proc. Eur. Conf. Optical Commun. (ECOC)*, (Basel, Switzerland), Sept. 2022. Paper Th1C.5.
12. C. Pehle and J. E. Pedersen, "Norse — A deep learning library for spiking neural networks," Jan. 2021. Documentation: https://norse.ai/docs/.
13. E. Müller, E. Arnold, O. Breitwieser, M. Czierlinski, A. Emmel, J. Kaiser, C. Mauch, S. Schmitt, P. Spilger, R. Stock, Y. Stradmann, J. Weis, A. Baumbach, S. Billaudelle, B. Cramer, F. Ebert, J. Göltz, J. Ilmberger, V. Karasenko, M. Kleider, A. Leibfried, C. Pehle, and J. Schemmel, "A scalable approach to modeling on accelerated neuromorphic hardware," *Front. Neurosci.*, vol. 16, 2022.
14. E.-M. Bansbach, A. von Bank, and L. Schmalen, "Spiking neural network decision feedback equalization," *arXiv preprint*, 2022.
15. F. Gardner, "A BPSK/QPSK timing-error detector for sampled receivers," *IEEE Trans. Commun.*, vol. 34, pp. 423–429, May 1986.